JOURNAL OF MATERIALS SCIENCE 12 (1977) 323–333

Coupled eutectic growth in Al-Fe alloys

Part 2 *Thermal stability of the Al-Al_6Fe eutectic*

I. R. HUGHES*, H. JONES
Department of Metallurgy, University of Sheffield, Sheffield, UK

The response to isothermal soaking at 773 to 913 K (0.83 to 0.99 T_m) for holding times up to 1000 h is reported for Al–3 wt % Fe/metastable Al–Al_6Fe eutectic (10 vol % Al_6Fe) directionally grown at 1.24 mm sec^{-1}. Breakdown is initiated by pinching-off and spherodization of Al_6Fe eutectic rods within eutectic cells and by growth of equilibrium Al_3Fe at grain boundaries and cell boundaries. Compared with equivalent Al–Al_3Ni, results indicate enhanced thermal stability of Al–Al_6Fe eutectic pending consumption by growing Al_3Fe. Hardness decreased with increased soaking time according to an Orowan relationship with Al_6Fe particle spacing.

1. Introduction

The prospect of employing eutectic composites for service at elevated temperatures has generated an expansion of interest in their thermal stability (see [1–3] for reviews). Cline [4] distinguished between (i) pinching-off and spherodization, (ii) two-dimensional coarsening, and (iii) fault migration, as mechanisms involved in thermal coarsening of fibrous eutectics. Although quantitative measurements of rates of coarsening have been reported for eutectics of Al–Al_3Ni [5–11], Al–Si [12], Fe–Fe_2B [13], NiAl–Cr [14, 15], NiAl–Mo [14] and Pb–Ag [16], limited information [8, 12] is available about the effect on thermal stability of a high (e.g. > 0.1 mm sec^{-1}) growth velocity in solidification, one of the means of extending or shifting the composition range of eutectic growth [17–22]. The subject of the present work, the Al–Al_6Fe rod eutectic, differs from those of earlier thermal stability studies in being *metastable*, requiring a high growth rate (> 0.1 mm sec^{-1}) in solidification for its formation and involving simultaneous coarsening of Al_6Fe and growth of equilibrium Al_3Fe at sufficiently high soaking temperatures. The conditions for growth of this eutectic have been reported in Part 1 [23].

2. Experimental procedure

Specimens for isothermal soaking were 3.2 mm diameter rods of Al–3.0 ± 0.1 wt % Fe prepared from superpurity (99.95%) aluminium and (99.8%) iron and longitudinally solidified at 1.24 mm sec^{-1} in a temperature gradient of 20 K mm^{-1} as described earlier [23]. Their structure was of Al–Al_6Fe eutectic with an Al_6Fe fibre spacing of 0.38 μm (8.0×10^6 rods per mm^2) as plate-like longitudinal cells of thickness ~40 μm. Specimens were soaked at temperatures between 773 and 913 K (0.83 to 0.99 T_m) held to ± 1 K for periods up to 1000 h. Specimens were sectioned and prepared for optical microscopy, scanning and transmission electron microscopy, X-ray diffraction and hardness testing as described before [23]. Counting of Al_6Fe rod number densities was performed on enlarged prints of scanning electron micrographs from deeply etched transverse sections. At least 1000, and typically > 5000 rods were counted to evaluate the number (N) per unit area. Hardness values were the average of at least twelve measurements on transverse sections made on Leitz equipment at 200 g load.

3. Results

3.1. Thermal coarsening and faceting of Al_6Fe

Fig. 1a to f are scanning electron micrographs showing the sequence of thermal coarsening of the

*Present address: Alcan International Ltd, Banbury, Oxon, OX6 7SP, UK.

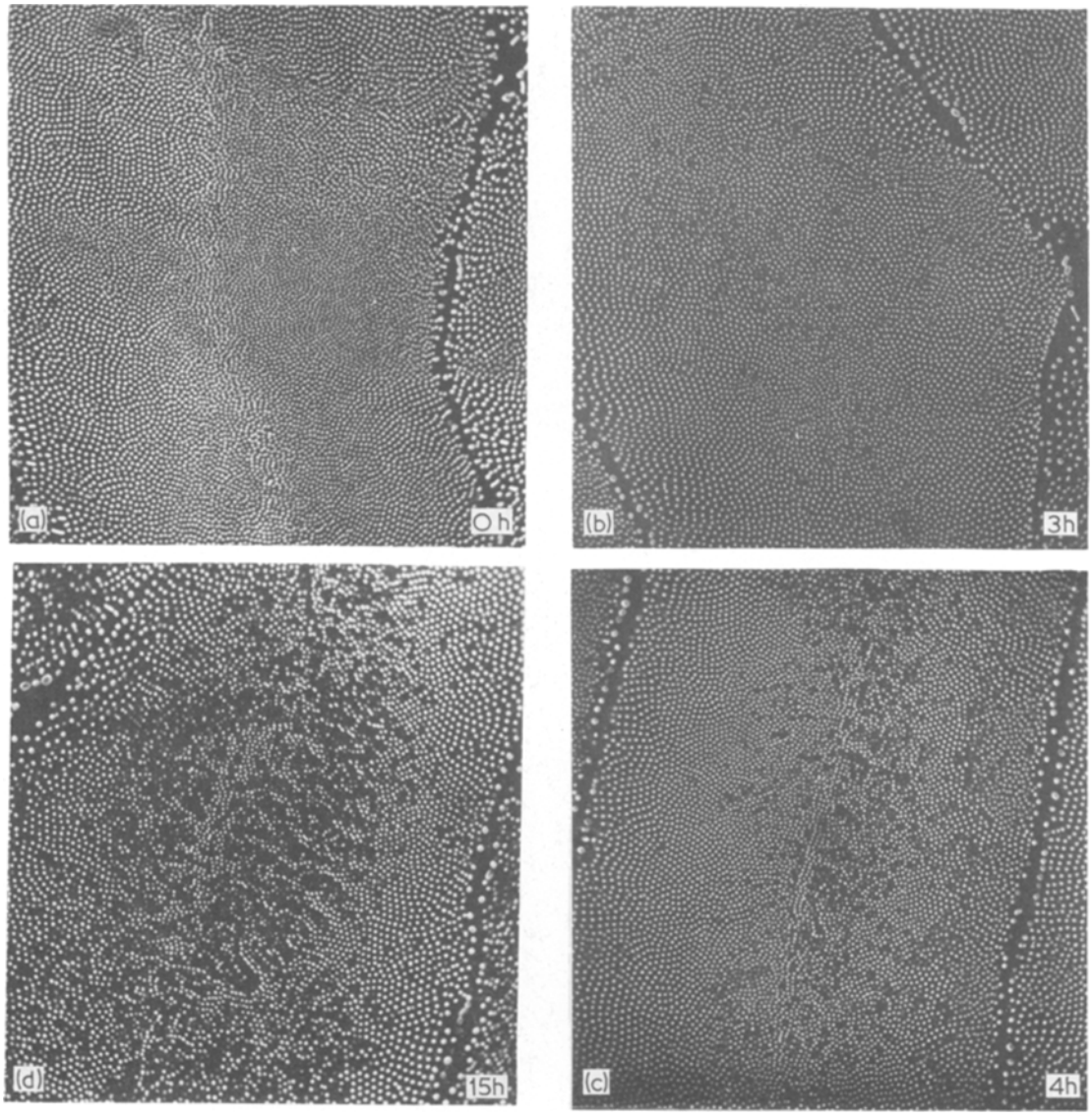

Figure 1 Scanning electron micrographs of deeply etched sections transverse to growth direction in solidification, showing progress of coarsening of Al–Al_6Fe eutectic during soaking at 773 K. (a) As-solidified, (b) to (f) after soaking for 3, 4, 15, 72 and 1001 h, respectively. × 2 100.

Al–Al_6Fe eutectic manifest as progressive disappearance of Al_6Fe fibres from transverse sections. This process commenced, or at least proceeded more rapidly, in regions at or near the centre of eutectic cells, spreading progressively towards the cell boundaries. Both observations accord with those of Smartt *et al.* [6, 9] by optical microscopy on Al–Al_3Ni eutectic solidified at a much lower velocity (0.028 mm sec^{-1}), in which fibre coarsening occurred preferentially in transverse bands associated with longitudinally misoriented fibres. Our observations on longitudinal sections, however, indicate that coarsening of Al_6Fe occurred by pinching-off or spherodization (Fig. 2a and b), as observed for Al–Al_3Ni [7], Al–Si [12], Cu–Cu_2O [26], Cu–Cu_2S [24], FeS–Fe [25] and NiAl–Cr [14], rather than by the two-dimensional coarsening process considered by Smartt *et al.* to be dominant for their Al–Al_3Ni [6].

Our results for the number of remaining Al_6Fe elements per unit area as a function of holding time at 773 and 873 K are given in Table I and in Fig. 6a and b. They show a decrease in N from 8

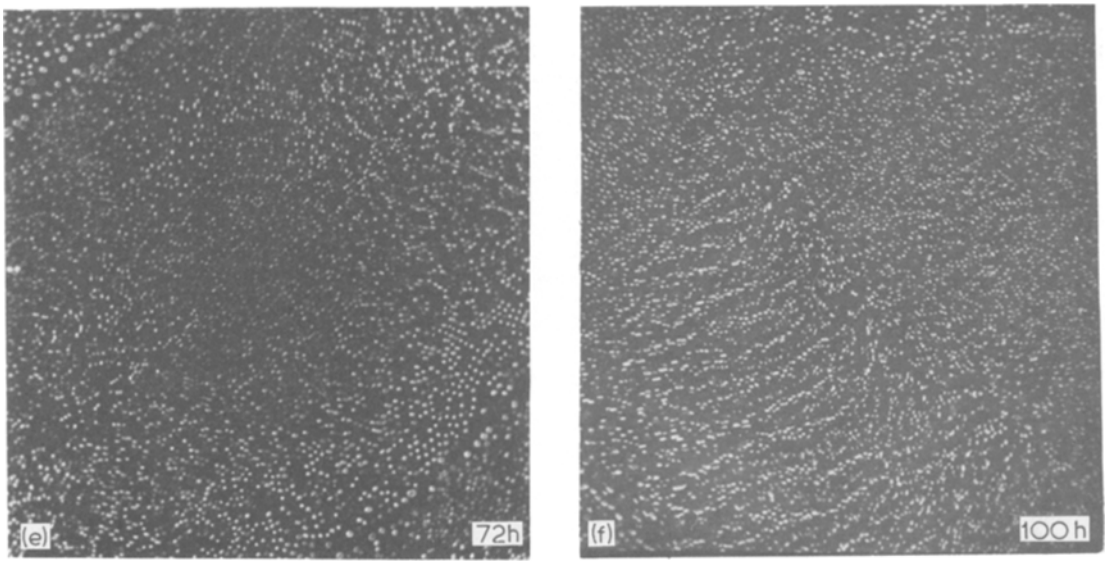

Figure 1 Continued.

TABLE I Remaining number N of Al_6Fe eutectic elements per unit area as a function of time at 773 and 873 K

Time at 873 K (h)	Number counted	N (μm^{-2})	Time at 773 K (h)	Number counted	N (μm^{-2})
0	15017	8.0 ± 0.5*	0	15017	8.0 ± 0.5*
2	5231	4.4	3	9284	9.0
3	1732	5.1	4	8535	8.8
4	4498	3.6	9	7087	7.0
9	8419	3.3	15	17153	6.5
160	11026	3.0	32	21603	5.1
250	5109	3.5	72	3512	4.6
			280	1654	5.0
			1000	12136	3.3

* Indicates bounds of scatter of measurements from nine separate areas.

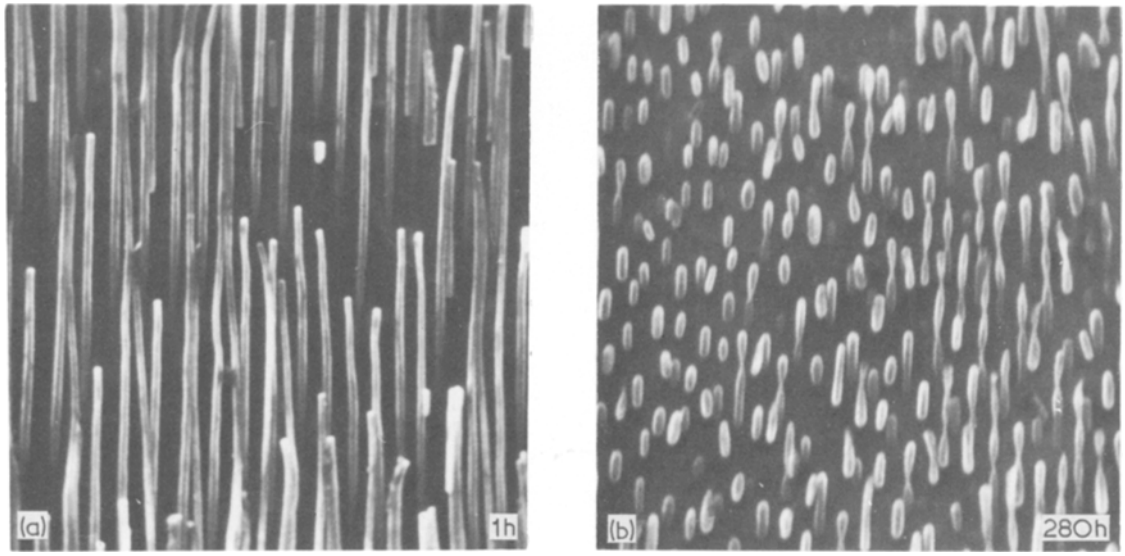

Figure 2 Mechanism of destabilization of Al_6Fe fibres by necking-down, pinching-off and spherodization on soaking at 773 K, after (a) 1 h, × 7 860; and (b) 280 h, × 7 750.

to $<4\,\mu m^{-2}$ in 1000 h at 773 K and in 250 h at 873 K, a small initial increase prior to this decrease being detected at 773 K. These measurements, transverse to the growth direction were taken well away from eutectic cell boundaries to avoid both the distorting effect of fibres inclined to the growth direction and inward progress of growing Al_3Fe (Section 3.2). This latter effect restricted measurements for 873 K to within 250 h beyond which remaining Al–Al_6Fe areas were too restricted to permit accurate counting. In spite of these precuations, the scatter in N-values is distinctly greater than in the equally careful measurements of Smartt *et al.* [6] on Al–Al_3Ni, doubtless reflecting the higher incidence of growth defects in our more rapidly solidified material.

Faceting of Al_6Fe was not pronounced in the as-solidified condition but developed strongly on soaking (Fig. 3a and b). While faceting is a normal feature of as-grown eutectics [26], NiAl–Cr being a notable exception [14], the effect has been shown to become less pronounced at high growth velocities and then requires subsequent thermal soaking to develop well-defined facets [27].

3.2. Discontinuous growth of equilibrium Al_3Fe

Concurrently with these morphological changes within the Al–Al_6Fe eutectic cells, discontinuous growth of equilibrium Al_3Fe occurred starting from eutectic grain boundaries (Fig. 4a) then spreading to cell boundaries (Fig. 4b). An intervening sheath of αAl separated these Al_3Fe platelets from adjacent unconsumed Al–Al_6Fe eutectic (Fig. 5a and b). Consumption of this eutectic had progressed little in 1001 h at 773 K (Fig. 5a) but was complete within 500 to 750 h at 873 K. There was evidence of nucleation and growth of Al_3Fe within cells in these later stages (Fig. 5b). Initiation of this process at boundaries was much less temperature-dependent than its completion, however, being detectable by optical microscopy after 4 to 5 h at 873 K and after 13 to 14 h at 773 K (Table II). This compares with less than 10 min at 823 K to form Al_3Fe from αAl supersaturated with 3.6 at.% (7.2 wt% Fe) by splat cooling [28, 29], an exposure some two orders of magnitude shorter

TABLE II Time for first appearance of Al_3Fe as a function of holding temperature

Temperature (K)	Time for first Al_3Fe (h)	Maximum time without Al_3Fe (h)
913	0.33*	0.25*
873	5*	4*
848	9	8
823	10	9
773	14	13

* Phase constitution confirmed by X-ray diffraction.

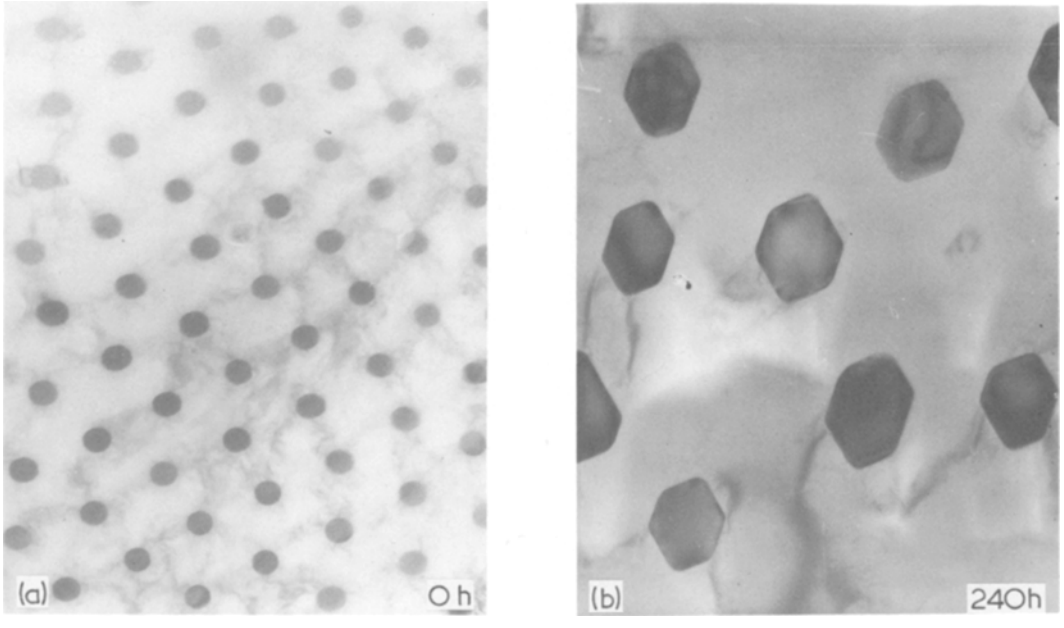

Figure 3 Transmission electron micrographs of sections transverse to growth direction in solidification, showing development of faceting of Al_6Fe during soaking. (a) As-solidified, × 21 500; (b) after 240 g at 773 K, × 61 300.

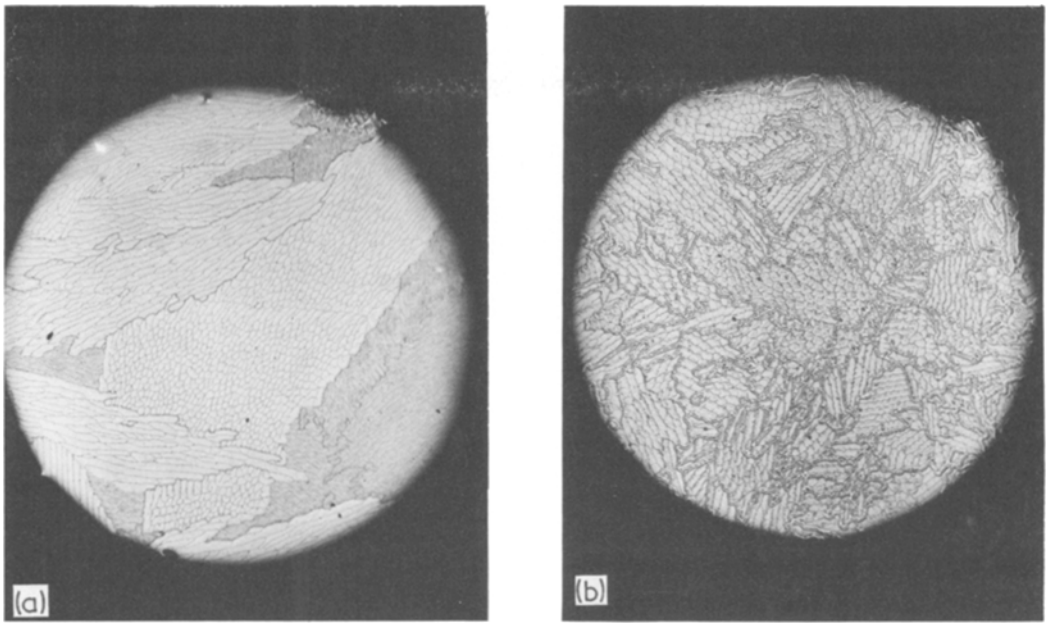

Figure 4 Optical micrographs of electroetched transverse sections, showing initiation of growth of Al_3Fe at Al–Al_6Fe eutectic grain boundaries then cell boundaries during soaking at 873 K. (a) After 5 h, and (b) after 201 h. × 18.6.

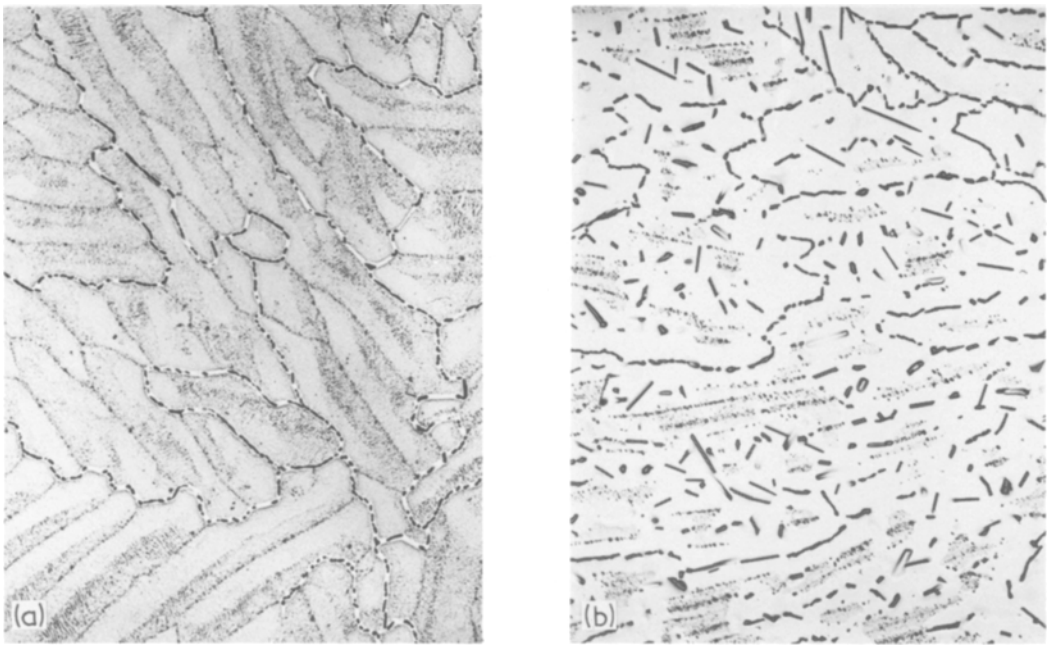

Figure 5 Optical micrographs of electro-etched transverse sections, showing mode of growth of Al_3Fe in Al–Al_6Fe eutectic by diffusion through a growing envelope of αAl during soaking. (a) After 1001 h at 773 K, × 129; and (b) after 500 h at 873 K, × 106.

than for our Al–Al_6Fe eutectic. A temperature of 473 K was required to form Al_3Fe within 15 h in these splats, 100 K lower than for the Al–Al_6Fe eutectic.

3.3. Hardness as a function of exposure time

Table III and Fig. 7 give hardness as a function of time of exposure at 773 and 873 K. The results for

TABLE III Microhardness (200 g load) as a function of time at 773 and 873 K

Time at 873 K (h)	Hardness ($kg\,mm^{-2}$)	Time at 773 K (h)	Hardness ($kg\,mm^{-2}$)
0	53.4	0	53.4
1	46.9	1	57.0
3	46.5	3	56.0
5*	47.3	5	54.4
9	46.9	9	54.0
24	46.3	11	51.7
64	44.1	15*	50.0
160	42.3	17	49.8
250	31.8	24	46.4
1006†	29.0	32	44.8
		72	44.3
		239	43.5
		1000	44.0

* Al_3Fe growth started
† Al_3Fe growth complete

773 K indicate an initial increase from 53 to 57 kg mm^{-2} decreasing to ~ 44 kg mm^{-2} during the first 32 h then remaining unchanged at least up to 1000 h. The initial stage up to 32 h included the start of Al_3Fe growth at boundaries and the reduction of Al_6Fe eutectic fibre density from 8 or 9 to 5 μm^{-2} thereafter remaining nearly constant up to 1000 h. The corresponding decrease to a plateau hardness value ~ 46.5 kg mm^{-2} occurred within the first hour at 873 K during which the Al_6Fe rod density decreased to a similar level. Significant further decreases in hardness were not detectable within 64 h and became marked only when substantial transformation to Al_3Fe had occurred at 250 and 1006 h.

4. Discussion

4.1. Mechanism of Al_6Fe eutectic fibre coarsening

Smartt *et al.* [6] identified three stages in the coarsening at 873 K of Al–Al_3Ni fibrous eutectic grown at 0.029 mm sec^{-1}, namely initial two-dimensional Ostwald ripening, during which N decreased from 0.65 to 0.22 μm^{-2} in the first 18 h, then remaining constant up to 48 h and finally decreasing steadily to 0.024 μm^{-2} in 768 h. This final stage was characterized as more rapid anisotropic two-dimensional Ostwald ripening developing increasingly non-equiaxed cross-sections in growing fibres. The intermediate transition stage was considered to result from a narrow initial distribution of fibre sizes and a low fault density continuing to delay the onset of the final anisotropic stage. Nakagawa and Weatherly [7], on the other hand, considered that fault migration rather than two-dimensional coarsening normally controls the coarsening of this eutectic even in the initial stages. Smartt *et al.* showed experimentally that increased initial fault density advanced the onset of anisotropic coarsening and Jones [30] showed that the reported effect of eutectic growth velocity on subsequent coarsening was consistent with a mean fault spacing proportional to initial fibre spacing λ_o, as found for lamellar eutectics.

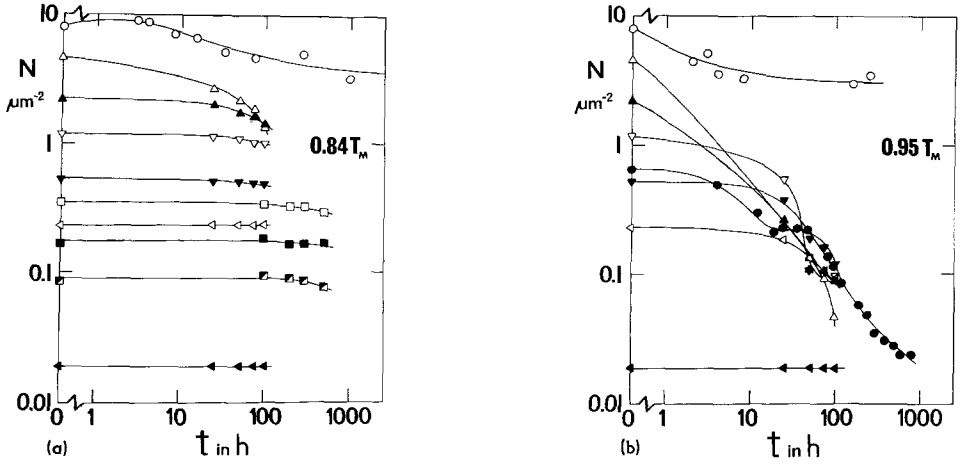

Figure 6 Number N of rods per unit area transverse to the growth direction as a function of holding time at (a) 773 and 781 K, and (b) 873 and 881 K, for various prior solidification velocities. Al–10 vol% Al_6Fe: ○ (present data from Table I) 1.24 mm sec^{-1}, (a) 773 K, (b) 873 K. Al–11 vol% Al_3Ni: ● (Smartt *et al.* [6]) 0.029 mm sec^{-1}, (a) no data (b) 873 K; △ 0.41, ▲ 0.19, ▽ 0.095, ▼ 0.045, ◁ 0.20 and ◀ 0.0017 mm sec^{-1} (Kurilo *et al.* [8]), (a) 781 K, (b) 881 K; □ 0.029, ■ 0.0136 and ▣ 0.0061 mm sec^{-1} (Bayles *et al.* [5]), (a) 781 K, (b) 881 K.

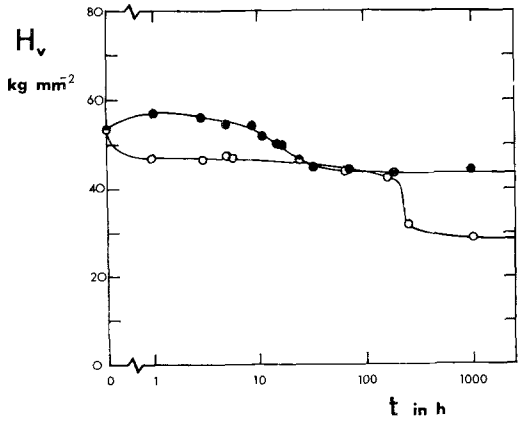

Figure 7 Hardness H_V as a function of a holding time, • 773 K, ○ 873 K.

The present results for Al–Al_6Fe eutectic grown at 1.24 mm sec^{-1} suggest that necking-down and pinching-off, the remaining mechanism suggested by Cline [4], assumes major importance for the highly faulted structure grown at this high solidification velocity. Adam and Jenkinson [12] reached the same conclusion for the thermally less stable Al–Si eutectic grown at 0.172 mm sec^{-1}, still a relatively high growth velocity. Capillarity theory predicts the time t_∞ to pinch-off a sphere from the end of an initially unperturbed rod radius r_o, to be

$$t_\infty = \beta r_o^n / K \qquad (1)$$

where for an interfacial diffusion mechanism [31], β is 6.54, n is 4, $K(=B)$ is $C_I D_I \gamma_I \Omega^2 \delta / kT$ where C_I and D_I are the concentration and diffusion coefficient of solute at the interface, γ_I is the interfacial energy, Ω is the atomic volume in the rod phase, δ is the interface thickness, k is Boltzmann's constant and T is temperature. No corresponding analytical calculation of β is available for a volume diffusion mechanism but McLean [32] evaluated β as 28.6 from measurements for rods of liquid lead in a solid aluminium matrix. In this case, n is 3, $K(=A)$ is $CD\gamma_I\Omega^2/kT$ where C and D are the solubility and diffusion coefficient of solute in the rod phase. For an initially perturbed rod, Jones [33] adapted and extended earlier calculations [4, 34] to obtain, for the rate of growth of perturbations:

$$dr/dt = K/\alpha\Lambda^2 r_o^{n-3} \qquad (2)$$

where $\alpha = \frac{1}{8}, \frac{1}{4}$ or $\frac{1}{45}$ for diffusion along the interface, in the rod phase or in the matrix, respectively, and Λ is the perturbation wavelength of maximum growth rate. Thus, to a first approximation:

$$t_\infty = \alpha\Lambda^2 r_o^{n-2}/K \qquad (3)$$

Assuming for the moment that volume diffusion in the matrix is the dominant mechanism of pinching-off for Al_6Fe rods in αAl, Equations 1 and 3 predict t_∞ as 5×10^8 and 1.1×10^5 h, respectively, at 773 K for our r_o of 0.63 μm and $\Lambda \sim 1$ μm, with A as 4×10^{-30} m^3 sec^{-1} calculated from C as 1.81×10^{24} atoms m^{-3} (solubility in aluminium of 0.003 at. % Fe at 773 K [35] and atomic volume of αAl as 16.6×10^{-30} m^3/atom [36]), D as 4.2×10^{-16} m^2 sec^{-1} at 773 K [37]*, γ_I as 0.225 J m^{-2} [38], Ω as 15.1×10^{-30} m^3/atom [39] and k as 1.38×10^{-23} J/atom K.

These values of t_∞ are, respectively, at least 6 and 3 orders of magnitude larger than the observed time of < 280 h for pinching-off Al_6Fe rods at 773 K. The observation of a t_∞ less than that predicted for unperturbed rods is expected, since the initial structure was highly faulted. Some possible explanations for the smaller overestimate of t_∞ for perturbed rods are:

(i) that the solubility used was the *equilibrium* value for Fe in αAl in the presence of Al_3Fe rather than the corresponding value applicable when metastable Al_6Fe is the second phase present. It is arguable that the value for Mn in Al (0.34 at. % Mn at 773 K [35]) in equilibrium with Al_6Mn (isomorphous with Al_6Fe) is a more accurate reflection of the solubility of Fe in αAl in the presence of Al_6Fe. Employing this value together with the larger D (1.3×10^{-15} m^2 sec^{-1} at 773 K) determined for Fe in Al by Alexander and Slifkin [40], the predicted values of t_∞ decrease to 2×10^6 and 300 h. This latter value for perturbed rods is then in much better agreement with our observations.

(ii) that the mass transport involved in pinching-off is dominated by interfacial diffusion rather than by bulk diffusion. The relative rates of growth $\dot{r}_I/\dot{r}$ of perturbations by the two mechanisms is given from Equation 2 as approximately $C_I D_I \delta / CDr_o$.

* This measured value lies between and within a factor of 2 to 3 of values extrapolated from higher temperature from the two other reliable determinations available [40, 41].

Although data on D_I for phase interfaces are scarce, values are available for $\alpha Al/Al_2Cu$ [42–44] and also Ag/Fe [45, 46]. The most recent reported result for Al/Al_2Cu [44] yields 2.8×10^{-8} m^2 sec^{-1} at 773 K, comparable with that extrapolated to this temperature from results [47] for grain-boundary diffusion in copper. Taking for the moment C_I equal to C then predicts $\dot{r}_I/r$ as ~ 500 (with δ as 5×10^{-12} m and D for Cu in Al at 773 K from Peterson and Rothman [48]) indicating predominance of interfacial diffusion. Its predominance is further increased if $C_I \to 1$ characteristic of strong interfacial adsorption of solute at interfaces and if D is for Fe in Al at 773 K.

While it is not certain whether (i) or (ii) is more significant in accounting for the observed t_∞, a limited solubility and low matrix diffusivity of Fe in Al would tend to favour the interfacial mass transport path compared, for example, with Si in Al [12] for which matrix diffusion was sufficient to account for the observed mass transport. Jones [33] concluded that interfacial diffusion could have made a significant contribution to spherodization of FeS–Fe and Cu–Cu_2S rod eutectics.

4.2. Rod coarsening of Al_6Fe compared with silicon and Al_3Ni in αAl

The rod perturbation growth rate at 773 K as high as 6×10^{-7} μm sec^{-1} indicated by Fig. 2b for Al_6Fe in αAl is some 200 times less than reported [12] for silicon rods in Al–Si eutectic at this temperature reflecting the higher stability of Al_6Fe to thermal coarsening. The time-dependences of the number N of rods per unit area remaining to intersect a random section (Fig. 6a and b) also indicates improved stability towards coarsening for Al_6Fe compared with Al_3Ni rods in αAl. Table I and Fig. 6a show for Al–10 vol% Al_6Fe solidified at 1.24 mm sec^{-1} ($\lambda_o = 0.4$ μm) that N/N_o after 1000 h at 773 K is 0.4 reached for Al–11 vol% Al_3Ni solidified at 0.41 mm sec^{-1} ($\lambda_o = 0.5$ μm) after only 75 h at the slightly higher temperature of 781 K [8]. Furthermore, while N/N_o for our Al_6Fe was relatively steady at 0.4 after 250 h at 873 K, N/N_o for Al–Al_3Ni solidified at 0.029 mm sec^{-1} ($\lambda_o = 1.3$ μm) was as small as 0.07 after a similar time (240 h) at the same temperature [6]. This evidently greater stability to coarsening of Al_6Fe is in spite of the fact that our Al–Al_6Fe had a higher solidification velocity than either of the Al–Al_3Ni samples and it is established ([5, 8, 30] and Fig. 6a and b) that increased prior solidification velocity leads to increased coarsening rates at a given holding temperature.

Equilibrium solid solubilities in the presence of Al_3Ni and Al_6Fe are identical for Ni and Fe in Al at 773 and 873 K [35] and therefore do not account for a difference in thermal stability. The possibly higher effective solid solubility (Section 4.1) for Fe in Al in the presence of Al_6Fe would thus tend to make Al_6Fe *less* stable to coarsening than Al_3Ni. Although no reliable measurement of D for Ni in Al is available [49], collected results [50] for diffusion of neighbouring transition metals in aluminium show systematic increases in D in the order Cr < Mn < Fe < Co > Cu at given temperatures up to 931 K. Although this value for Cu [48] is slightly less than that for Co [40], the value for Ni would have to be greater than that for Fe to maintain the sequence. Such a regular sequence is well-established, for example, for diffusion of these transition metals in iron [51]. While confirmation that D for Ni exceeds that for Fe in aluminium would, at least partially, account for a higher stability of Al_6Fe to coarsening, another possibility is that diversion of diffusing iron from coarsening Al–Al_6Fe eutectic areas to feed growth of Al_3Fe at cell boundaries, could result in a reduced coarsening rate for the remaining Al_6Fe. This effect would be greater at 873 K for which substantial Al_3Fe growth occurred in the time-scale of the Al_6Fe coarsening measurements.

The well-defined plateau in N at 3.3 ± 0.3 m^{-2} for Al–Al_6Fe grown at 1.24 mm sec^{-1} for the time interval 4 h up to at least 250 h at 873 K is reminiscent of that found [6] for relatively unfaulted Al–Al_3Ni grown at 0.029 mm sec^{-1} for the time interval 18 h to 48 h at the same temperature, prior to operation of a final stage, considered to be two-dimensional coarsening in that case. Intervention of discontinuous growth of Al_3Fe at 873 K precluded investigation of any equivalent final stage (three-dimensional Ostwald ripening) in the present study of Al–Al_6Fe. The small increase in N recorded for the first 3 h at 773 K (Table I and Fig. 6a) and also reflected in an increase in H_V (Table III and Fig. 7), however, is similar to effects on N detected for Al–Al_3Ni at 781 K [5] and at 898 K [7]. These small initial increases in N during coarsening could possibly be a result of pinching-off side-branches at junctions between rods. This would lend support to the interpretation [7] that

those particular Al–Al_3Ni samples coarsened primarily by fault migration rather than by two-dimensional coarsening.

4.3. Growth of Al_3Fe at boundaries

The progressive growth in Al–3 wt% Fe/Al–Al_6Fe eutectic of equilibrium Al_3Fe at cell and grain boundaries requires an incubation time of 10 h at 823 K (Table II and Section 3.2) compared with less than 10 min for first appearance of Al_3Fe at this temperature in Al–7.2 wt% Fe supersaturated αAl solid solution made by splat cooling [28]. Similarly, a temperature 100 K higher was required to form Al_3Fe within a given time from the Al–Al_6Fe eutectic compared with the extended solid solution. This mainly reflects the difference that Al_3Fe forms by *continuous* precipitation *within* the αAl grains [51] for the solid solution rather than by *discontinuous* precipitation at grain and cell boundaries for the Al–Al_6Fe eutectic. It is clear that prior dissolution of a fine-grained second phase in the solid solution occurs more readily than dissolution of relatively coarse Al_6Fe rods in the eutectic, favouring a grain or cell boundary nucleated decomposition for the eutectic coarsening simultaneously within the grains and cells. It is interesting to note that a grain boundary nucleated decomposition does occur concurrently with Al_3Fe precipitation within the grains of solid solution but this involves growth of non-equilibrium Al_6Fe that eventually dissolves in favour of equilibrium Al_3Fe [52]. The conclusion would seem to be that Al_6Fe has difficulty nucleating within the solid solution in competition with Al_3Fe while Al_3Fe does not nucleate readily on or within Al_6Fe eutectic rods.

4.4. Relation between hardness and microstructure resulting from coarsening

The decreases of hardness from 53 or 57 to 44 kg mm^{-2} in 1000 h at 773 K and to 42 kg mm^{-2} in 160 h at 873 K (Table III and Fig. 7) correspond to decreases in number of Al_6Fe rods per unit area from 8 or 9 to 3 μm^{-2} (Table I and Fig. 6). Adam and Jenkinson [12] attributed the declining fracture strength of thermally coarsened Al–Si fibrous eutectic to a combination of Hall–Petch strengthening from the αAl grain size and Orowan strengthening from the dispersed silicon particles. Fig. 8 shows hardness plotted against $S^{-1}\log_{10}S$ conforming to an Orowan relationship [53] of the form

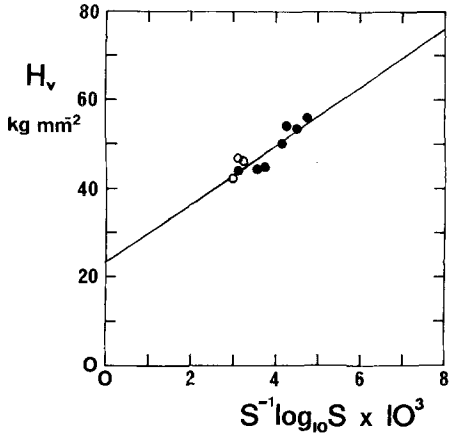

Figure 8 Hardness H_V as a function of Orowan parameter $S^{-1}\log_{10}S$, where S is distance L in the matrix separating neighbouring particles divided by twice the Burgers vector b. • 773 K, ○ 873 K.

$$\tau_o = \frac{G}{4\pi}\frac{1}{S}\log_e S \qquad (3)$$

in which τ_o is the critical resolved shear stress, G is the matrix shear modulus and S is $L/2b$ where b is the Burgers vector (taken to be 2.86×10^{-10} m for aluminium) and L ($\sim N^{-\frac{1}{2}}$) is the interphase spacing. Hardness is related to τ_o noting that H_V is $3.0\,\sigma_o$ for full plasticity [54] and, on the basis of the Von Mises criterion [54], that σ_o is $3\tau_o$ so that, in general terms

$$H_V = H_o + JS^{-1}\log_{10}S \qquad (4)$$

where J ($= (9G/4\pi)\log_{10}e$) is the slope and H_o is the intercept of a graph of H_V against $S^{-1}\log_{10}S$. The least squares line shown in Fig. 8 for the available data points taken from Tables I and III yields an intercept H_o of 23.1 ± 4.3 kg mm^{-2} and a slope $J = 6700 \pm 1100$ kg mm^{-2}. Using data of Carreker and Hibbard [55] for aluminium, the eutectic cell size of 40 μm should make a Hall–Petch contribution of up to 3 kg mm^{-2} to the flow stress equivalent to a contribution of up to 9 kg mm^{-2} to H_o. Taking G for aluminium as 2560 kg mm^{-2} [56] yields a theoretical J of 4200 kg mm^{-2} compared with the experimental value of 6700 kg mm^{-2} from Fig. 8. This agreement within a factor of ~2 between prediction and measurement for both H_o and J is in line with results of earlier related comparisons [53, 55] and is considered to be reasonable taking into account assumptions in the theory, approximations in its application and experimental scatter in the present case.

5. Conclusions

(1) Thermal decomposition of Al–10 vol % Al_6Fe rod eutectic grown at 1.24 mm sec^{-1} occurs by growth of Al_3Fe from eutectic cell and grain boundaries and simultaneously by pinching-off and spherodization of Al_6Fe eutectic rods within eutectic cells.

(2) The kinetics of pinching-off Al_6Fe eutectic rods at 773 K are more consistent with control by interfacial diffusion than by lattice diffusion.

(3) The greater apparent stability to coarsening of Al_6Fe compared with Al_3Ni rods at 773 and 873 K may to some extent reflect a diversion of diffusing iron to feed growth of Al_3Fe at cell boundaries as well as a lower diffusion coefficient in aluminium for iron.

(4) The decrease in hardness from 53 to 57 to 44 kg mm^{-2} in 1000 h at 773 K and to 42 kg mm^{-2} in 160 h at 873 K corresponding to a reduction in Al_6Fe particle density from 8 or 9 to 3 μm^{-2}, is reasonably consistent with an Orowan relationship.

Acknowledgements

The authors are grateful to Professors G. W. Greenwood and B. B. Argent for providing laboratory facilities and to the Science Research Council for supporting one of us (IRH).

References

1. M. J. SALKIND, in "Interfaces in Composites", ASTM Spec. Publ. 452, Philadelphia Pa. (1969) p. 149.
2. G. C. WEATHERLY, in "Directionally Solidified *In-Situ* Composites", NATO/AGARD Conf. Proc. 156, edited by E. R. Thompson and P. R. Sahm (1974) p. 13, and in "Treatise on Materials Science", Vol. 8, edited by H. Herman (Academic Press, New York, 1975). p. 121.
3. A. LAWLEY, in "New Industries and Applications for Advanced Materials Technology", Proceedings of the 19th National Symposium, Buena Park, California (1974) p. 424.
4. H. E. CLINE, Acta Met. **19** (1971) 481.
5. B. J. BAYLES, J. A. FORD and M. J. SALKIND, *Trans. Met. Soc. AIME* **239** (1967) 844.
6. H. B. SMARTT, L. K. TU and T. H. COURTNEY, *Met. Trans.* **2** (1971) 2717.
7. Y. G. NAKAGAWA and G. C. WEATHERLY, *Acta Met.* **20** (1972) 345.
8. Yu. P. KURILO, A. I. SOMOV and A. S. TORTIKA, *Phys. Met. Metallogr.* **34** (6) (1972) 161.
9. H. B. SMARTT and T. H. COURTNEY, *Met. Trans.* **4** (1973) 217; **7A** (1976) 123.
10. G. GARMONG and T. H. COURTNEY, *ibid* **6A** (1975) 1945.
11. D. R. H. JONES and G. J. MAY, *Acta Met.* **23** (1975) 29.
12. C. McL. ADAM and D. C. JENKINSON, in "Metallurgy in Australasia", edited by J. S. Smaill (Australian Instutute of Metals, Melbourne, 1974) p. 58.
13. A. R. T. De SILVA and G. A. CHADWICK, *Met. Sci. J.* **6** (1972) 157.
14. J. L. WALTER and H. E. CLINE, *Met. Trans.* **4** (1973) 33.
15. G. C. MAY, *Metal Sci.* **9** (1975) 269.
16. D. R. H. JONES, *Mater. Sci. Eng.* **15** (1974) 203.
17. J. D. HUNT and K. A. JACKSON, *Trans. Met. Soc. AIME* **239** (1967) 864.
18. H. E. CLINE and J. D. LIVINGSTON, *ibid* **245** (1969) 1987.
19. R. S. BARCLAY, H. W. KERR and P. NIESSEN, *J. Mater. Sci.* **6** (1971) 1168.
20. H. A. H. STEEN and H. HELLAWELL, *Acta Met.* **20** (1972) 363.
21. C. McL. ADAM and L. M. HOGAN, *J. Austral. Inst. Met.* **17** (1972) 81.
22. J. A. EADY, L. M. HOGAN and P. G. DAVIES, *ibid* **20** (1975) 23.
23. I. R. HUGHES and H. JONES, *J. Mater. Sci.* **11** (1976) 1781.
24. S. MARICH and D. JAFFREY, *Met. Trans.* **2** (1971) 2681.
25. S. MARICH, *ibid* **1** (1970) 2953.
26. L. M. HOGAN, R. W. KRAFT and F. D. LEMKEY, in "Advances in Materials Research", Vol. 5, edited by H. Herman (Wiley-Interscience, New York 1971) p. 83.
27. G. GARMONG, C.G. RHODES and R.A. SPURLING, *Met. Trans.* **4** (1973) 707.
28. A. TONEJC and A. BONEFAČIĆ, *J. Appl. Phys.* **40** (1969) 419.
29. A. TONEJC, *Met. Trans.* **2** (1971) 437.
30. H. JONES, *Scripta Met.* **8** (1974) 1011.
31. F. A. NICHOLS and W. W. MULLINS, *J. Appl. Phys.* **36** (1965) 1826.
32. M. McLEAN, *Phil. Mag.* **27** (1973) 1253.
33. D. R. H. JONES, *J. Mater. Sci.* **9** (1974) 989.
34. F. A. NICHOLS and W. W. MULLINS, *Trans. Met. Soc. AIME* **233** (1965) 1840.
35. M HANSEN and K. ANDERKO, "Constitution of Binary Alloys" (McGraw-Hill, New York, 1958).
36. P. RUDMAN, *Trans. Met. Soc. AIME* **233** (1965) 871.
37. G. P. TIWARI and B. D. SHARMA, *Phil. Mag.* **24** (1971) 739.
38. C. McL. ADAM, Ph.D. Thesis, University of Queensland (1971).
39. L. K. WALFORD, *Acta Crystallogr.* **18** (1965) 287.
40. W. B. ALEXANDER and L. M. SLIFKIN, *Phys. Rev.* **B1** (1970) 3274.
41. G. M. HOOD, *Phil. Mag.* **21** (1970) 305.
42. H. B. AARON and H. J. AARONSON, *Acta. Met.* **16** (1968) p. 789.
43. J. GOLDMAN, H. I. AARONSON and H. B. AARON, *Met. Trans.* **1** (1970) 1805.
44. E. HO and G. C. WEATHERLY, *Acta Met.* **23** (1975) 1451.
45. A. BONDY, P. REGNIER and V. LEVY, *Scripta Met.* **5** (1971) 345.
46. B. JOB, J. MATHIE and P. REGNIER, *Acta Met.* **22**

(1974) 1197.
47. B. BURTON and G. W. GREENWOOD, *Metal Sci. J.* **4** (1970) 215.
48. N. L. PETERSON and S. J. ROTHMAN, *Phys. Rev.* **B1** (1970) 3264.
49. M. BISHOP and K. E. FLETCHER, *Int. Met. Rev.* **17** (1972) 203.
50. G. M. HOOD and R. J. SCHULTZ, *Phil. Mag.* **23** (1971) 1479.
51. C. D. MORTON, Ph.D. Thesis, University of Sheffield (1975).
52. M. H. JACOBS, A. G. DOGGETT and M. J. STOWELL, *Fizika* **2** (1970) 18.1; *J. Mater. Sci.* **9** (1974) 1631.
53. M. F. ASHBY, *Z. Metallk.* **55** (1964) 5.
54. G. E. DIETER, "Mechanical Metallurgy", (McGraw-Hill, New York, 1961).
55. R. P. CARREKER and W. R. HIBBARD, *Trans. Met. Soc. AIME* **209** (1957) 1157.
56. P. M. SUTTON, *Phys. Rev.* **91** (1953) 816.

Received 18 May and accepted 14 June 1976.